

# Quantitative Testing of Robustness on Superomniphobic Surfaces by Drop Impact

Thi Phuong Nhung Nguyen,<sup>†,‡</sup> Philippe Brunet,<sup>\*,‡</sup> Yannick Coffinier,<sup>†</sup> and Rabah Boukherroub<sup>†</sup>

<sup>†</sup>Institut de Recherche Interdisciplinaire (IRI) USR CNRS 3078, Université Lille Nord de France - Parc de la Haute Borne 50 Avenue de Halley, BP 70478, 59658 Villeneuve d'Ascq, Cedex, France, and <sup>‡</sup>Institut d'Electronique de Microélectronique et de Nanotechnologies (IEMN) UMR CNRS 8520, Université Lille Nord de France, Avenue Poincaré, BP 60069, 59652 Villeneuve d'Ascq, France

Received August 3, 2010. Revised Manuscript Received September 24, 2010

The quality of a liquid-repellent surface is quantified by both the apparent contact angle  $\theta_0$  that a sessile drop adopts on it and the value of the liquid pressure threshold the surface can withstand without being impaled by the liquid, hence maintaining a low-friction condition. We designed surfaces covered with nanowires obtained by the vapor–liquid–solid (VLS) growth technique that are able to repel most of the existing nonpolar liquids including those with very low surface tension as well as many polar liquids with moderate to high surface tension. These superomniphobic surfaces exhibit apparent contact angles ranging from 125 to 160° depending on the liquid. We tested the robustness of the surfaces against impalement by carrying out drop impact experiments. Our results show how this robustness depends on Young's contact angle  $\theta_0$  related to the surface tension of the liquid and that the orientational growth of nanowires is a favorable factor for robustness.

## I. Introduction

The fabrication of water-repellent surfaces is nowadays commonly achieved by a host of different techniques.<sup>1–8</sup> It is admitted that a micro- or nanotextured surface with an appropriate low-energy coating is able to repel water. Although the early studies on superhydrophobicity were undertaken on surfaces consisting of regular arrays of micrometer-scale posts,<sup>1,2</sup> the current state of the art benefits from recent improvements in nanotexturation by chemical growth, for instance, silicon nanowires (SiNWs) or carbon nanotubes.

However, most of the liquid-repellent surfaces are effective only for high-surface-tension ( $\gamma$ ) liquids such as water. The current challenge in their applicability in lab-on-a-chip microfluidics or in high-performance clothes is to design surfaces that repel liquids of lower surface tension. Recent achievements by Tuteja et al.<sup>9,10</sup> employ surfaces with overhanging roughness elements, denoted as “re-entrant”, with a regular array of mushroom-shaped posts. Other kind of substrates<sup>11–13</sup> with less-regular texture also achieved high repellency with low- $\gamma$  liquids.

In this article, we present quantitative results for a new type of superomniphobic surface composed of tangled silicon nanowires

(SiNWs) coated with a low-surface-energy fluoropolymer whose fabrication details are given later. Figure 1 displays a scanning electron microscopy (SEM) image of a drop of polyphenyl-methylsiloxane (Aldrich) with a low surface tension ( $\gamma = 24.5$  mN/m) that was deposited and dried to become solid on one of our surfaces. A contact angle of about 120° was measured with such a wetting liquid. Figure 1b shows a magnified view close to the contact line, which provides evidence of the repelling character of the SiNWs: the drop sits on top of them.

What defines a good super-repellent surface is the largest possible apparent contact angle (CA) with a small contact angle hysteresis (CAH), typically  $\theta_a - \theta_r \leq 5^\circ$ , but also its ability to retain a state of small CAH when large external forces are applied to the liquid; hereafter, we denote this property as “robustness”. The condition for a small CAH is achieved when the liquid–vapor interface is weakly impaled or not impaled in the texture. Once impaled, the liquid remains stuck: the retention force and the CAH increase dramatically, which is not suitable for applications of low-friction drop displacement or self-cleaning, and this is most likely to happen for low-surface-tension liquids. Therefore, one of the remaining questions is how the robustness depends on the nature of the liquid. Our study addresses this issue by measuring the impalement pressure threshold  $P_c$  for liquids with various  $\gamma$  using drop impact experiments.

## II. Qualitative Analysis of the Robustness of a Surface

It is well established that the roughness induces a modification of the apparent macroscopic CA  $\theta$ . To be more precise, the Cassie–Baxter approach assumes that the drop sits on top of the roughness elements, leading to the following expression for the apparent angle<sup>14</sup>

$$\cos \theta = \phi_s(\cos \theta_0 + 1) - 1 \quad (1)$$

(14) Cassie, A.; Baxter, S. *Trans. Faraday Soc.* **1944**, *40*, 546.

\*To whom correspondence should be addressed. E-mail: philippe.brunet@univ-lille1.fr.

- (1) Bico, J.; Marzolin, C.; Quéré, D. *Europhys. Lett.* **1999**, *47*, 220–226.
- (2) Herminghaus, S. *Europhys. Lett.* **2000**, *52*, 165–170.
- (3) Lau, K. K. S.; Bico, J.; Teo, K. B. K.; Chhowalla, M.; Amaratunga, G. A. J.; Milne, W. I.; McKinley, G. H.; Gleason, K. K. *Nano Lett.* **2003**, *3*, 1701.
- (4) Patankar, N. A. *Langmuir* **2004**, *20*, 8209.
- (5) Gao, L.; McCarthy, T. J. *Langmuir* **2006**, *22*, 2966.
- (6) Nosonovsky, M. *Langmuir* **2007**, *23*, 3157–3161.
- (7) Verplanck, N.; Galopin, E.; Camart, J. C.; Thomy, V.; Coffinier, Y.; Boukherroub, R. *Nano Lett.* **2007**, *7*, 813.
- (8) Verplanck, N.; Coffinier, Y.; Thomy, V.; Boukherroub, R. *Nanoscale. Res. Lett.* **2007**, *2*, 577–596.
- (9) Tuteja, A.; Choi, W.; Ma, M.; Mabry, J. M.; Mazzella, S. A.; Rutledge, G. C.; McKinley, G. H.; Cohen, R. E. *Science* **2007**, *318*, 1618–1622.
- (10) Tuteja, A.; Choi, W.; Mabry, J. M.; McKinley, G. H.; Cohen, R. E. *Proc. Natl. Acad. Sci. U.S.A.* **2008**, *105*, 18200–18205.
- (11) Cao, L. L.; Price, T. P.; Weiss, M.; Gao, D. *Langmuir* **2008**, *24*, 1640–1643.
- (12) Ramos, S. M. M.; Benyagoub, A.; Canut, B.; Jamois, C. *Langmuir* **2010**, *26*, 5141–5146.
- (13) Liu, Y.; Xiu, Y.; Hess, D. W.; Wong, C. P. *Langmuir* **2010**, *26*, 8908–8913.

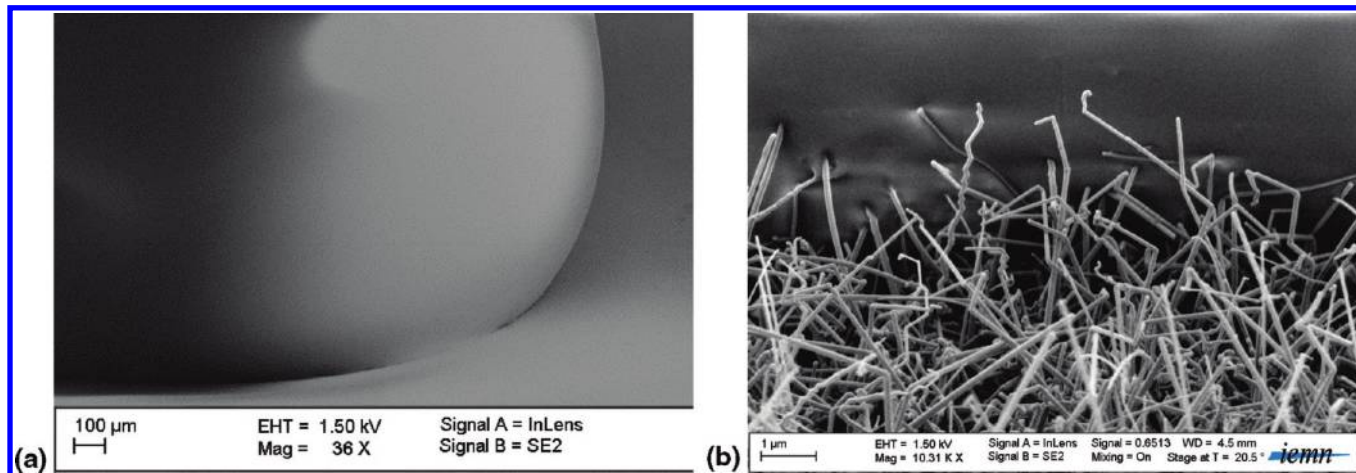


**Figure 1.** (a) Drop of a dried polymer (polyphenyl-methylsiloxane,  $\gamma = 24.5$  mN/cm) on a carpet of SiNWs. (b) Enlarged image under the drop, evidencing the Cassie–Baxter state.

where  $\phi_s$  is the surface fraction of the liquid–solid interface and  $\theta_0$  is Young’s contact angle obtained on a perfect smooth surface. The Wenzel approach assumes that the liquid completely fills the space between the texture elements. Under this assumption, the apparent CA equals<sup>15</sup>

$$\cos \theta = r \cos \theta_0 \quad (2)$$

where  $r$  is the surface roughness (i.e., the ratio between the total surface and the projected one ( $r \geq 1$ )). Equation 2 suggests that the roughness leads to a large apparent CA, provided that  $\theta_0$  is larger than  $\pi/2$ , and eq 1 suggests that large  $\theta$  values are obtained with a texture of thin wires and a large pitch. However, eqs 1 and 2 do not give any clue about which state is more favorable under the given external conditions, the fakir one (Cassie–Baxter) or the impaled one (Wenzel). By simple arguments on surface energy,<sup>16</sup> one can evaluate a critical Young’s angle  $\theta_{0c}$  as

$$\cos \theta_{0c} = -\frac{1 - \phi_s}{r - \phi_s} \quad (3)$$

If  $\theta_0 \geq \theta_{0c}$ , then the surface energy of the Cassie–Baxter state is lower than that of the Wenzel state: the drop stands on top of the texture. The condition  $\theta_0 \geq \theta_{0c}$  is generally not fulfilled for low- $\gamma$  liquids. However, it is possible to keep a liquid–vapor interface in a weakly impaled state even when  $\theta_0 \geq \theta_{0c}$ . This is related to the metastable character of the Cassie–Baxter state: in a free-energy landscape, this state can be located at a local minimum whereas the free energy is often located at a global minimum in the Wenzel state.<sup>6,17</sup> Furthermore, it has been recently shown<sup>10,17</sup> that a metastable Cassie–Baxter state can be achieved even if  $\theta_0 \leq \pi/2$ , provided that the roughness elements have an overhanging shape. This peculiar geometry allowed for low- $\gamma$  liquid-repellent surfaces. The robustness against impalement is then related to the height of the energy barrier between the two limit states.

Drop impact experiments are a particularly versatile way to test this robustness.<sup>18–22</sup> During impact, the sudden vertical deceleration of the liquid particles leads to momentum transfer that applies an effective dynamic pressure of  $P_{\text{dyn}} = \frac{1}{2}\rho U^2$ , with  $U$  being the impact velocity and  $\rho$  being the liquid density. The value of this pressure is easily determined by measuring  $U$  just before impact, and the pressure peak is localized at the center of impact, hence enabling the test of impalement over a reduced area. Furthermore, it has been shown<sup>18</sup> that this dynamic pressure is equivalent to a static one for liquid impalement. In other words, there are no dynamic effects involved during the droplet penetration in the texture, which ensures the universal character of the results obtained by this method.

Most of the superomniphobic surfaces that have been designed are made of an ordered texture with roughness elements with size ranging from a few micrometers to a few tens of micrometers.<sup>9,10</sup> According to Washburn’s law for pressure entry in porous media,<sup>23</sup> the order of magnitude of the entry pressure is inversely proportional to the typical size  $R$  of the roughness:  $P_w = 2\gamma \cos(\theta)/R$ . The quantitative measurements obtained on periodic arrays of micropillars showed that  $R \approx s^2/L$ ,<sup>18,19</sup> where  $s$  and  $L$  stand for the space between the pillars and their length, respectively. Therefore, our idea is to increase the robustness by covering the surface with a forest of chemically grown SiNWs with high aspect ratios (from 30 to 100) that are about 50 to 100 nm in diameter (Figure 2). This texture scale is still hardly accessible by current lithography and etching techniques: the realization of surfaces larger than about 1 cm<sup>2</sup> is expensive and time-consuming. However, this texture scale is more simply and cheaply achievable with the chemical growth of silicon NWs. To ensure the equivalence of the reentrant geometry of surfaces used in refs 9 and 10, we used growth parameters (pressure, temperature, etc.) in order to get disordered and multidirectional wires growing diagonally (Figure 2). The downside of this disorder is that there does not exist an obvious characterization of their roughness or their surface fraction.

### III. Preparation of Superomniphobic Substrates by Chemical Vapor Deposition (CVD)

The silicon NWs are synthesized on a silicon substrate by using the vapor–liquid–solid (VLS) growth mechanism as described in more detail in refs 7 and 20. A 300 nm SiO<sub>2</sub> layer is deposited thermally on the silicon substrate, coated with a 40 Å layer of

(15) Wenzel, R. *Ind. Eng. Chem.* **1936**, *28*, 988.  
 (16) Quéré, D. *Rep. Prog. Phys.* **2005**, *68*, 2495.  
 (17) Marmur, A. *Langmuir* **2008**, *24*, 7573–7579.  
 (18) Bartolo, D.; Bouamirène, F.; Verneuil, E.; Buguin, A.; Silberzan, P.; Moulinet, S. *Europhys. Lett.* **2006**, *74*, 299.  
 (19) Reyssat, M.; Pepin, A.; Marty, F.; Chen, Y.; Quéré, D. *Europhys. Lett.* **2006**, *74*, 306.  
 (20) Brunet, P.; Lapière, F.; Coffinier, Y.; Thomy, V.; Boukherroub, R. *Langmuir* **2008**, *24*, 11203–11208.  
 (21) Tsai, P.; Pacheco, S.; Pirat, C.; Lefferts, L.; Lohse, D. *Langmuir* **2009**, *25*, 12293–12298.  
 (22) Lapière, F.; Brunet, P.; Coffinier, Y.; Thomy, V.; Blossey, R.; Boukherroub, R. *Faraday Disc.* **2010**, *146*, 125–139.

(23) Washburn, E. W. *Phys. Rev.* **1921**, *17*, 273.

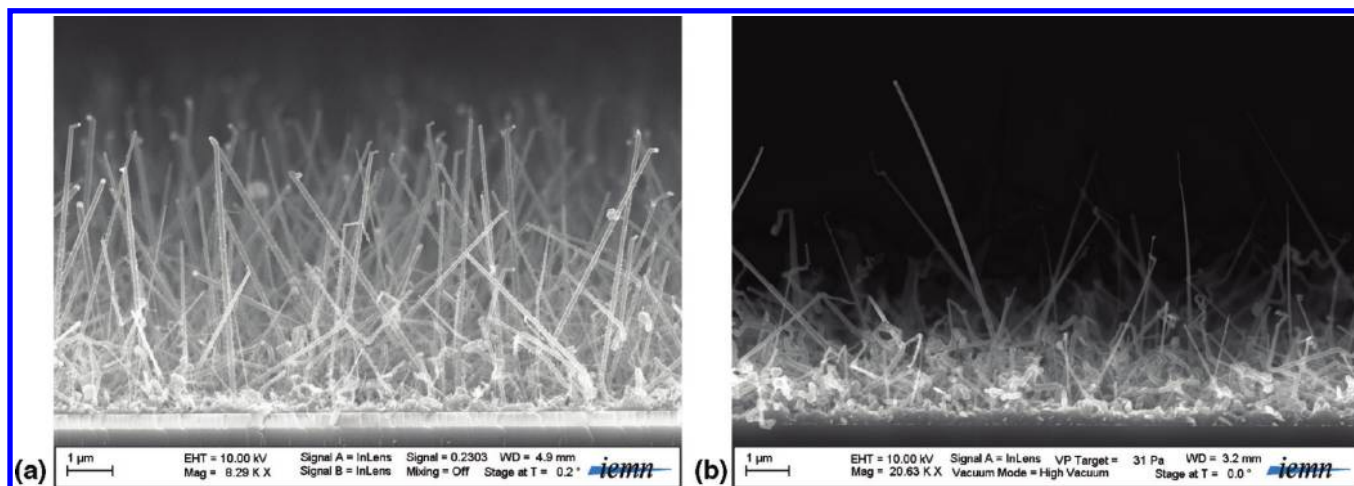


**Figure 2.** SEM images of the NW surfaces prepared by the VLS growth technique. (a)  $P = 0.4$  Torr and 10 min “VLS 1”. (b)  $P = 0.1$  Torr and 60 min “VLS 2”.

gold, and then placed in an oven. The substrate is heated to  $500\text{ }^{\circ}\text{C}$ , forming gold nanoparticles acting as catalysts for silicon NW growth. Then, silane gas ( $\text{SiH}_4$ ) is injected following its preferential decomposition on gold. The  $\text{SiH}_4$  molecules dissociate and silicon atoms are incorporated into the gold droplet, forming a AuSi liquid eutectic. This induces the directional growth of a NW with the gold nanoparticle on top. The NW’s width, length, and morphology depend on the duration, the pressure, and the temperature of the process as well as on the crystal orientation of the silicon substrate.<sup>24</sup> The  $\text{SiO}_2$  layer ensures relative disorder in the diagonal direction of the NW growth. The orientation is also influenced by the pressure prescribed during the VLS process:<sup>25</sup> the orientation varies from about  $30$  to  $90^{\circ}$  with respect to the horizontal: the larger the pressure, the straighter the NWs grow (also with a narrower orientation distribution).

Two surfaces have been used in this study corresponding to different growth conditions on a p-type (boron-doped) silicon wafer, leading to different morphologies. The first process, hereafter denoted as VLS1, has a duration of 10 min with a pressure of  $0.4$  Torr (T). The nanotexture is shown in Figure 2a: it consists of one-layered texture of  $7\text{-}\mu\text{m}$ -length NWs. Their average orientation is about  $80^{\circ}$  with respect to the horizontal plane. (The smaller orientation angle of the few NWs at the forward plan is due to the fact that they have been broken during the cutting of the surface prior to SEM imaging.) The second process, hereafter denoted as VLS2, has a duration of 60 min at a pressure of  $0.1$  T. The nanotexture is shown in Figure 2b. It comprises a dense lower layer made of  $\sim 2\text{ }\mu\text{m}$  short entangled NWs and a few NWs of  $7\text{ }\mu\text{m}$  in length. The orientation is more irregular than for VLS1, and the average angle with the horizontal is smaller. Some of them even have a “hook” shape on their top end.

The as-prepared SiNW surface is hydrogen-terminated. However, upon exposure to air, a thin native oxide layer is formed on the surface. This termination confers a superhydrophilic character to the surface with a contact angle close to zero.<sup>26</sup> Therefore, because of its high roughness, all of the tested liquids perfectly wet the surface, as predicted by the Wenzel equation (eq 2). To turn the surfaces superomniphobic, they are coated

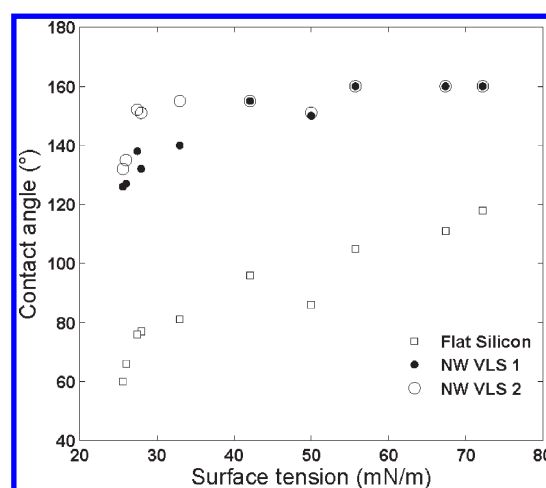


**Figure 3.** Contact angle on flat silicon, NW VLS1, and NW VLS2 surfaces vs  $\gamma$ .

**Table 1. Physical Properties of the Investigated Liquids**

liquid	$\pi$ ( $\text{g}/\text{cm}^3$ )	$\nu$ ( $\text{mm}^2/\text{s}$ )	$\gamma$ ( $\text{mN}/\text{m}$ )
water	1.00	1.00	72.2
water + glyc 50/50	1.126	4.93	67.4
water + Et 95/5	0.988	1.42	55.73
$\text{CH}_2\text{I}_2$	3.32	2.26	50.0
water + Et 85/15	0.973	2.23	42.08
water + Et 70/30	0.951	2.47	32.98
water + Et 50/50	0.910	2.20	27.96
hexadecane	0.77	3.90	27.47
water + Et 38/62	0.882	1.98	26.02
water + Et 35/65	0.871	1.89	25.61

with 1H,1H,2H,2H-perfluorodecyltrichlorosilane (PFTS), a low-surface-energy layer. The PFTS molecules are dissolved in hexane, and the surfaces are immersed in the solution for 6 h at room temperature in a dry-nitrogen-purged glovebox. The resulting surface was rinsed with hexane, chloroform, and isopropanol and dried with a gentle stream of nitrogen.

#### IV. Wetting Properties

We investigated liquids with surface tension varying from 25 to 72  $\text{mN}/\text{m}$ . Liquids of lower  $\gamma$ , such as *n*-hexane, spontaneously invade the NW texture. For each liquid (Table 1), the CA and

(24) Lapiere, F.; Thomy, V.; Coffinier, Y.; Blossey, R.; Boukherroub, R. *Langmuir* **2009**, *25*, 6551–6558.

(25) Kawashima, T.; Mizutani, T.; Nakagawa, T.; Torii, H.; Saitoh, T.; Komori, K.; Fujii, M. *Nano Lett.* **2008**, *8*, 362–368.

(26) Coffinier, Y.; Janel, S.; Addad, A.; Blossey, R.; Gengembre, L.; Payen, E.; Boukherroub, R. *Langmuir* **2007**, *23*, 1608–1611.

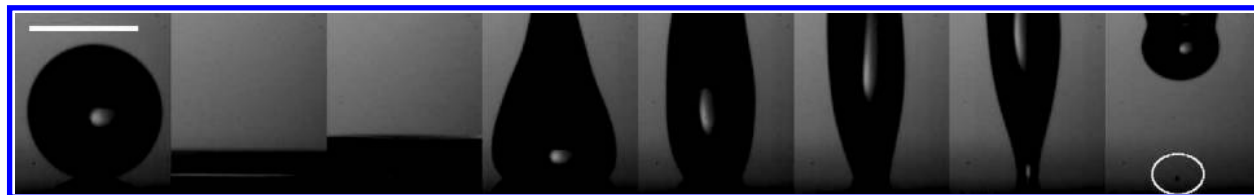


**Figure 4.** Typical sequence of liquid impalement (here diiodomethane  $\text{CH}_2\text{I}_2$  on the VLS2 surface). A small drop remains, testifying to the vicinity of the threshold (inside the white circle), as the drop bounces off the surface. The time between each snapshot is 2.67 ms. The bar in the first snapshot scales to 1 mm.

CAH on smooth silicon, NW-VLS1, and NW-VLS2 surfaces are measured with a goniometer (DSA100, Kruss GmbH Germany) and plotted in Figure 3 versus surface tension. The contact angle  $\theta_0$  of the drop on a smooth (flat) silicon surface is an appropriate measurement of the wettability of the surface for a given liquid. Indeed, the sole surface tension  $\gamma$  between the liquid and its vapor cannot fully define this wettability because the surface tension between the liquid and the solid  $\gamma_{\text{SL}}$  is not a priori known or measurable. Although  $\theta_0$  on flat silicon decreases continuously as  $\gamma$  decreases (with a CAH ranging from 20 to 30°), the CA on the two NWs surfaces shows a plateau at about 160° and a small hysteresis (about 1°) for high- $\gamma$  liquids, hence ensuring superomniphobic behavior. A sharp decrease in  $\theta$  below 140° occurs at a threshold for  $\gamma$ . This threshold is about 33 mN/m for VLS1 and 26 mN/m for VLS2. However, despite the fact that the CA can fall to 125°, the CAH remains weak (around a few degrees), which testifies that the drop remains in a Cassie–Baxter state. In most cases, VLS2 offers the best repelling performance.

### V. Test of Robustness: Drop Impact Experiments

The setup we used for drop impact has been previously presented in more detail.<sup>20,22</sup> We used a dripping faucet that releases a drop of liquid from a submillimetric nozzle. The drop detaches from the nozzle as the action of gravity overcomes the capillary retention forces. Therefore, the diameter of the drop is determined by the capillary length of the liquid and is very reproducible. Again, the properties of the liquids tested are given in Table 1. The height of the fall  $h$  prescribes the velocity at impact,  $V_0 = (2gh)^{1/2}$ , which can be up to 5.5 m/s. Using back-lighting together with a high-speed camera (at a maximal rate of 4700 frames/s with a resolution of  $576 \times 576$ ), the shape of the interface during the spreading and bouncing processes can be determined. The magnification allows for an accuracy of about 8  $\mu\text{m}$  per pixel.

When released on a superomniphobic surface, a drop of any tested liquid deforms and spreads like a pancake then retracts and bounces off the surface, as previously observed in details.<sup>18–22</sup> To determine  $P_c$ , we increase the height of the fall  $h$  (or impact velocity  $U$ ) until the tiniest visible amount of liquid remains at the impact location during the bouncing phase: this is observed in a typical sequence as in Figure 4. It is important to notice that the viscosity of the liquid  $\nu$  strongly influences the dynamics of the spreading and bouncing phase: while the use of a nonviscous liquid such as water sometimes leads to the atomization of the main drop into many smaller droplets during the spreading phase (especially at a high impact velocity), using large- $\nu$  liquids induces a large amount of dissipation within the texture. As a consequence, even if the drop has not been impaled on the texture down to the bottom (Wenzel state), the large viscous dissipation prevents the liquid from escaping the texture because the bouncing height is lower than the size of the elongated drop. Therefore, we chose moderately viscous liquids, on the order of a few  $\text{mm}^2/\text{s}$ , to avoid the undesirable aforementioned effects.

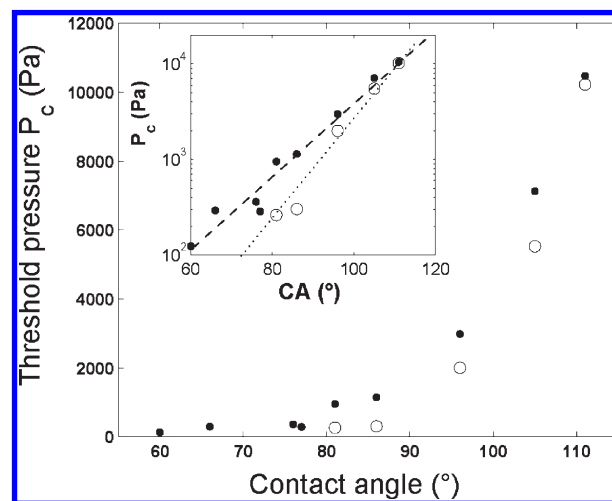


**Figure 5.** Pressure threshold for liquid impalement vs Young's contact angle  $\theta_0$  in which a drop of liquid adopts an equivalently smooth surface. The open symbols stand for the VLS1 surface, and the filled symbols stand for the VLS2 surface. (Inset) Linear log plot.

It must also be mentioned that we attempted impalement experiments induced by droplet evaporation, in the same spirit as in refs 18 and 27 in order to compare the obtained threshold with that measured with drop impact. However, because of the very low hysteresis (1 to 2°), it was very hard to maintain a drop on our surfaces. The slightest departure from the horizontal or the weakest wind made the drop unexpectedly roll off the surface, which made it difficult to carry out such experiments.

Figure 5 shows the threshold pressure  $P_c$  versus the contact angle on flat silicon  $\theta_0$ . Whatever the liquid used, the threshold is always higher for the VLS2 surface than for the VLS1 surface. The pressure  $P_c$  goes to zero for CA  $\theta_0$  smaller than 60° and seems to grow exponentially with  $\theta_0$  (inset). This plot is the confirmation of the high robustness of NW surfaces against liquid impalement, even for low- $\gamma$  liquids. However, this robustness tends to deteriorate for highly wetting liquids, and there is a limiting surface tension (or  $\theta_0$ ) below which the liquid drop is spontaneously impaled by the texture. This means that the capillary pressure itself is large enough to overcome the pressure threshold:  $P_c \leq 2\gamma/R$ . Above this limit in  $\theta_0$ , the pressure threshold sharply increases: the growth can roughly be fitted by an exponential law (Figure 5).

From Figure 5, it is clear that the VLS2 surface is more robust than the VLS1 surface. This fact suggests that straight vertical NWs do not offer the best robustness and that a rough, disordered lower layer should better improve the robustness. However, it is not possible to account quantitatively for the influence of surface

(27) Tsai, P.; Lammertink, R. G. H.; Wessling, M.; Lohse, D. *Phys. Rev. Lett.* **2008**, *104*, 116102.

roughness and the influence of NW orientation on the robustness and to discriminate between the effects of these two factors.

This is clearly at odds with what was expected from previous measurements of  $P_c$  with water on superhydrophobic surfaces: a dense structure of tall, thin posts or NWs clearly have an advantage for larger  $P_c$  values.<sup>18–20</sup> We also conducted experiments with another type of surface with even more vertically oriented NWs (the same as that denoted as “P3” in ref 20), and the robustness was even worse than for VLS1. We did not mention these experiments here because of the aging of the surface (i.e., the formation of “bundles” of NWs similar to what was observed in carbon nanotubes (see Figure 6 in ref 3) prevented reproducible experiments). Therefore, our results reveal that it is crucial to have diagonally grown NWs in order to get a good robustness for low- $\gamma$  liquids.

## VI. Conclusions

We presented the first quantitative measurements of the robustness of a superomniphobic surface. We measured the pressure threshold for liquid impalement on two different NW surfaces for various liquids with different surface tension, which allowed us to test the influence of the Young’s contact angle  $\theta_0$  that a liquid

drop adopts on a smooth surface with the same surface energy. It turns out that  $\theta_0$  plays a crucial role in robustness: for a surface with a given structure and roughness, there exists a threshold value for  $\theta_0$  below which one observes the spontaneous impalement (without drop impact) of a liquid. Above this threshold in  $\theta_0$ , the limiting pressure sharply increases with  $\theta_0$ .

Surfaces made of a carpet of nanowires, oriented with a finite angle with respect to the vertical, offered liquid-repellent character with very good robustness over a large range of  $\gamma$  and a nanoscale equivalent of the re-entrant structures proposed in previous studies.<sup>9,10</sup> However, it is not yet clear whether it is the average orientation or the relative disorder of the NWs that contributes to better robustness. Future studies will be focused on elucidating these points.

**Acknowledgment.** We are indebted to the BioMems team of IEMN for the technical support that was required to carry out this experimental study. The European Community’s Seventh Framework Programme (FP7/20072013) under grant agreement no. 227243, the Centre National de la Recherche Scientifique (CNRS), and the Nord-Pas-de Calais region are gratefully acknowledged for financial support.